



LES OF SEPARATED FLOWS AT MODERATE REYNOLDS NUMBERS APPROPRIATE FOR TURBINE BLADES AND UNMANNED AERO VEHICLES

F. Cadiuex, G. Castiglioni, J. A. Domaradzki

Department of Aerospace and Mechanical Engineering
University of Southern California
Los Angeles, California 90089-1191
cadioux@usc.edu; castigli@usc.edu;
jad@usc.edu

T. Sayadi, S. Bose

Center for Turbulence Research
Stanford University
Stanford, California, 94305
sayadi@ladhyx.polytechnique.fr;
stbose@stanford.edu

M. Grilli, S. Hickel

Lehrstuhl für Aerodynamik und Strömungsmechanik
Technische Universität München
Boltzmannstr. 15
85748 Garching b. München
Muzio.Grilli@aer.mw.tum.de; sh@tum.de

ABSTRACT

Flows over airfoils and blades in rotating machinery, for unmanned and micro-aerial vehicles, wind turbines, and propellers consist of a laminar boundary layer near the leading edge that is often followed by a laminar separation bubble and transition to turbulence further downstream. Typical RANS turbulence models are inadequate for such flows. Direct numerical simulation (DNS) is the most reliable but is also the most computationally expensive alternative. This work assesses the capability of LES to significantly reduce the resolution requirements for such flows and still provide results of DNS quality. Two flows are considered. A flow over a flat plate with suitable velocity boundary conditions away from the plate to produce a separation bubble and a 2-D flow on a NACA-0012 airfoil. By employing several different codes we conclude that accurate LES are possible using $O(1\%)$ of the DNS resolution and that the numerical dissipation plays a significant role in LES of such flows.

INTRODUCTION

The physical origin of laminar and transitional flow separation is qualitatively well understood: the attached laminar boundary layer developing on a wing or blade is subjected to an adverse pressure gradient due to the airfoil's curvature, which causes it to separate. Immediately behind the separation point there is an effectively stagnant flow region, the so-called dead air region, followed by a reverse flow vortex. The interface between the separated flow moving away from the wing and the recirculating flow in the vicinity of the wing results in a shear layer with an inflectional mean velocity profile. This shear layer experiences Kelvin-Helmholtz instabilities that develop into turbulence after first generating characteristic spanwise vortices. Further downstream, the separated turbulent flow reattaches and gradually evolves into the classical turbulent bound-

ary layer. The separation bubble's shape and size changes in time due to vortex shedding, making the problem inherently unsteady. The above picture emerges from numerous experimental investigations, e.g. Marxen *et al.* (2003); Hu *et al.* (2007); Hain *et al.* (2009), and Spedding & McArthur (2010), as well as from direct numerical simulations (DNS) results by Lin & L.Pauley (1996); Spalart & Strelets (2000); Alam & Sandham (2000); Marxen & Rist (2010); Jones *et al.* (2008), and Jones *et al.* (2010).

Low to moderate Reynolds number separation driven by an adverse pressure gradient as opposed to geometry is an intrinsically non-equilibrium process. It involves subtle interactions between viscous, advective, and pressure effects that can only be reliably captured by solving the full Navier-Stokes equations, i.e. using DNS. However, DNS require substantial computational resources, e.g. Jones *et al.* (2008) used over 170 million grid points for a relatively simple 3-D configuration. If a DNS approach is not feasible other simulation options must be considered. RANS methods commonly used and optimized for high Reynolds number turbulent flows were tested by Spalart & Strelets (2000) and shown to be inadequate for the separated flows of interest. Another option is to employ large eddy simulation (LES) techniques. For instance, Yang & Voke (2001) reported LES results obtained with the dynamic Smagorinsky in good agreement with experiments for boundary-layer separation and transition caused by surface curvature at $Re = 3,450$. Yet even for this relatively low Reynolds number, the critical issues in getting agreement was a good numerical resolution (2×10^6 mesh points), comparable to DNS of the same flow, and a high order numerical method. Similarly, Eisenbach & Friedrich (2008) performed LES of flow separation on an airfoil at a high angle of attack at $Re = 10^5$ using Cartesian grids, getting a good agreement with experimental results. However, this case also required very high resolutions between

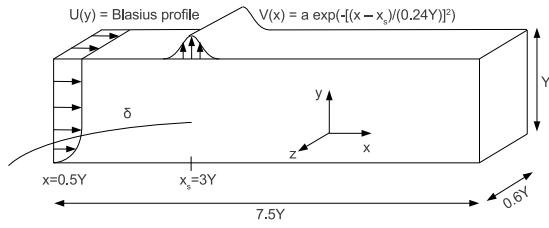


Figure 1. Physical domain, boundary and inlet conditions used to investigate laminar separation bubble flow

50 and 100 million mesh points. A rare example of low resolution LES is given by Almutairi *et al.* (2010). In that study results for a laminar separation bubble over an airfoil at $Re = 5 \times 10^5$ are in good agreement with Jones *et al.* (2008) at 4.5% of DNS resolution. Therefore, the question remains: can LES produce sufficiently accurate results for laminar separation bubble flows with drastically reduced resolution, around 1% of DNS resolution, commonly achievable for fully turbulent flows?

BENCHMARK FLOWS AND NUMERICAL METHODS

A procedure used successfully by other investigators (Wilson & Pauley, 1998; Alam & Sandham, 2000; Spalart & Strelets, 2000) to induce separation in a flow over a flat plate is followed. As seen in Fig. 1, the computational domain is a rectangular box of height Y with a rigid lower wall on which the boundary layer flow evolves. A laminar Blasius boundary layer velocity profile with the free stream velocity U_0 is imposed at the inflow. At the top boundary, a vertical suction velocity is imposed in a narrow slot oriented perpendicular to the mean flow direction. The suction produces an adverse pressure gradient that causes flow separation. The flow then transitions to turbulence and reattaches.

Following Spalart & Strelets (2000) the vertical suction velocity is specified as

$$V(x) = a \exp(-[(x - X_s)/(0.24Y)]^2), \quad (1)$$

where a is the peak velocity and X_s is its streamwise location. The resulting separation bubble is sensitive only to the upper-wall boundary conditions through the nominal flow deceleration parameter S ,

$$S = \frac{1}{YU_0} \int V(x) dx. \quad (2)$$

Spalart & Strelets (2000) chose the location of the peak suction velocity as $X_s = 3Y$ and set $S = 0.3$ and the Reynolds number at X_s to $Re_X = 10^5$, giving $a \approx 0.7U_0$ and $Re_Y = Re_X/3$. These choices are driven by the requirement that the flow separates naturally, without additional forcing mechanisms.

The numerical code, made available by CTR/Stanford, solves full compressible Navier-Stokes equations for a perfect gas using sixth-order compact finite differences (Nagarajan *et al.*, 2007). An implicit-explicit time integration scheme is applied. For explicit time advancement, a

Table 1. Resolution and parameters for CTR simulations. N is the number of grid points.

	CTR DNS	CTR LES	CTR UDNS
$N_{total} \times 10^6$	59.0	2.3	0.7
% of DNS	100	3.9	1.2
Δx^+	9.7	26.4	57.0
Δy^+ at $x = 7$	0.5	1.0	1.6
Δz^+	7.6	27.5	29.6

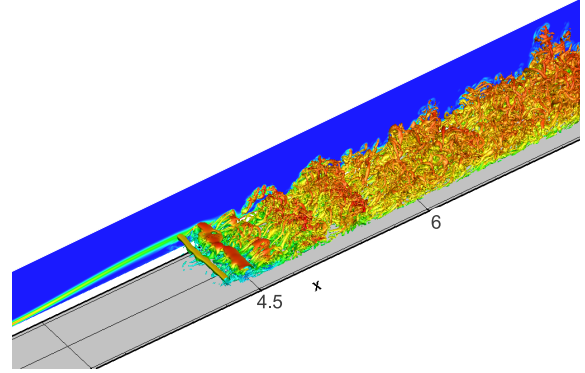


Figure 2. CTR DNS snapshot of iso-surfaces of vorticity: Kelvin-Helmholtz rolls are visible over the separated shear layer leading to transition to turbulence and subsequent turbulent flow reattachment, closing of the separation bubble.

third-order Runge-Kutta scheme (RK3) is employed and a second-order A-stable scheme is used for the implicit portion. Compact filtering as described by Lele (1992) is employed at each time step, both in the freestream and wall-normal directions to ensure overall stability and zonal matching at the interface between the implicit and explicit grids (Nagarajan, 2004). The numerical scheme is constructed on a structured curvilinear grid, and the variables are staggered in space. The spanwise direction is treated as periodic. Numerical sponges (Mani, 2012) are used at all other boundaries, except at the rigid bottom wall, to ensure that sound and vortical waves are not reflected back into the computational domain. The freestream Mach number is chosen to be 0.2. Results from three simulations are reported here: a DNS benchmark case (CTR DNS), a wall-resolved LES with the dynamic Smagorinsky model (CTR LES), and a highly under-resolved DNS (CTR UDNS). Parameters for these simulations are summarized in Table 1 and the flow is illustrated in fig. 2.

The specific geometrical setting for the second benchmark flow is that of a NACA-0012 airfoil at $Re_c = 5 \times 10^4$ at 5 deg of incidence for which detailed DNS results were obtained by Jones *et al.* (2008, 2010). Our simulations are performed using a numerical code INCA developed at TUM and a standard commercial code STAR-CCM+ available from CD-adapco.

INCA solves the compressible three-dimensional Navier-Stokes equations in a conservative form, using as a SGS model the Adaptive Local Deconvolution Method (ALDM) that has shown to be a reliable, accurate, and efficient method for implicit LES of Navier-Stokes turbulence (Hickel *et al.* (2006); Hickel & Larsson (2008)). For discretization INCA uses Cartesian grids, which facilitate

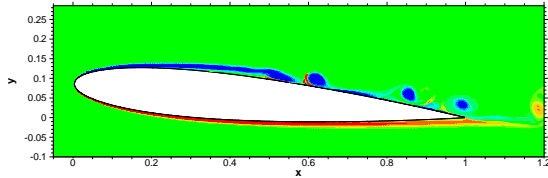


Figure 3. 2-D iso-countours of spanwise vorticity using 10 levels over the range $\pm 75 \omega^+$ for INCA.

automatic grid generation and adaptive local grid refinement by dyadic sub-partitioning. Cartesian grids also imply fewer computational operations per grid point than body-fitted or unstructured grids. On the other hand, geometric boundaries do not necessarily coincide with grid lines, so that boundary conditions have to be applied at the subcell level. INCA implements a conservative immersed boundary method for representing sharp interfaces between a fluid and a rigid body on Cartesian grids, see Meyer *et al.* (2010); Grilli *et al.* (2009). The viscous stresses at the fluid-solid interface are approximated by linear differencing schemes. The interface pressure is obtained by solving the one-sided (symmetric) Riemann problem in the interface-normal direction. Characteristic boundary conditions of Poinso & Lele (1992); Lodato *et al.* (2008) are applied at the far-field domain boundaries. At the downstream exit boundary, which will be subject to the passage of nonlinear fluid structures, a low value for the reflection parameter has been set. These boundary conditions avoid unphysical reflections that could strongly influence the flow in the vicinity of the airfoil. As the scheme operates on fluxes only, this cut-cell FV method maintains accuracy and ensures mass and momentum conservation. Discrete conservation and a sharp representation of the fluid-solid interface render this method particularly suitable for LES of turbulent flows.

STAR-CCM+ similarly solves the compressible three-dimensional integral Navier-Stokes equations in conservative form. The equations are solved in a preconditioned dimensional form on an unstructured grid CD-adapco (2013). The time is advanced through a dual time-stepping implicit scheme. The inviscid fluxes are evaluated by using the Weiss-Smith preconditioned Roe's flux-difference splitting scheme which is formally at best second order accurate. The viscous fluxes are evaluated by a standard central difference scheme. Two different SGS explicit models are available in the code: dynamic Smagorinsky (Germano *et al.*, 1991; Lilly, 1992) and wall-adapting local eddy viscosity model (WALE) (Nicoud & Ducros, 1999). Both have been implemented in the present work.

So far only 2-D simulations have been performed and analyzed. Given the inherently 3-D nature of turbulence it is obvious that 2-D simulations cannot be used to judge the quality of the LES models. On the other hand they provide a good calibration test for the simulations methodology and for estimating grid resolution required in 3-D cases. In 2-D laminar flows the ALDM scheme does not provide a turbulence model, but it simply acts as a slightly dissipative, 2nd order accurate centered discretization. Therefore the results presented should be considered as under-resolved DNS. Parameters for these simulations are summarized in Table 2 and the flow is illustrated in Fig. 3.

Table 2. Summary of 2-D time averaged LSB characteristics. N is the number of grid points, x_s the separation point, x_r the reattachment point and l_b the length of the bubble.

Simulation	Model	$N \times 10^6$	x_s	x_r	l_b
Jones <i>et al.</i>	DNS	1.6	0.152	0.582	0.430
INCA	ALDM	0.22	0.179	0.623	0.444
STAR-CCM+	UDNS	0.1	0.142	0.590	0.448
STAR-CCM+	WALE	0.1	0.151	0.581	0.430
STAR-CCM+	Dyn. Smag.	0.1	0.153	0.581	0.428

EVALUATION METRICS

As quantitative metrics to assess various methods we use the pressure coefficient, $C_p = (p - P)/\frac{1}{2}\rho U^2$, and the friction coefficient, $C_f = \tau_w/\frac{1}{2}\rho U^2$, at the surface (P is the free stream pressure, U the free stream velocity, and τ_w the wall stress). Both quantities are averaged over time. The friction coefficient is particularly useful in determining the location and extend of the separation bubble as it has a negative sign in the regions of a reversed flow. The benchmark data are results obtained in high resolution DNS (CTR DNS, and Jones *et al.* (2008)).

The wall pressure coefficients shown in Fig. 4 for the flat plate case for the under-resolved DNS and LES are both in good agreement with the DNS benchmark with the exception of a slight difference in bubble length. The downward slope in C_p in Fig. 5 after $x = 5$ indicates the existence of a slight favorable pressure gradient which extends to the end of the physical domain. Although weak, the favorable pressure gradient may also artificially improve agreement of LES and UDNS results with the DNS benchmark because of its effect on the reattachment location.

At resolutions on the order of 1% of their respective benchmark DNS, and even without models, all simulations predict the separation point seen in DNS benchmarks exactly. This can be observed in the first zero-crossing on the wall skin friction plots in Fig. 5. The UDNS predicts the shape and maximum value of the peak negative skin friction almost exactly. Wall-resolved LES with dynamic Smagorinsky modeling performs slightly worse than the UDNS run, but still reaches within 15% of the DNS peak negative skin friction coefficient value. UDNS and LES predict the location of the reattachment point with less than 5% difference with the DNS. UDNS recovers almost exactly the turbulent C_f in the region downstream of the bubble whereas LES results never recover completely.

For 2-D NACA-0012 airfoil flow all simulations have been run for at least 17 times units, c/U , where c is the cord length and U is the free stream velocity, and were averaged over the last 10 time units before plotting. Quantitative comparison for the pressure coefficient, shown in Fig. 6 is fairly good. Regarding INCA, the pressure side (positive C_p) comparison is excellent, although this is expected since the boundary layer on the lower side of the airfoil is fully laminar. The suction side (negative C_p), however, is not completely satisfactory since the second peak in pressure after the plateau generated by the presence of the bubble is not resolved. Similar behavior can be observed in the skin friction comparison (Fig. 7). The pressure side (a line above the zero line) is well captured, with the exception of the peaks, which is a sign of insufficient resolution in that

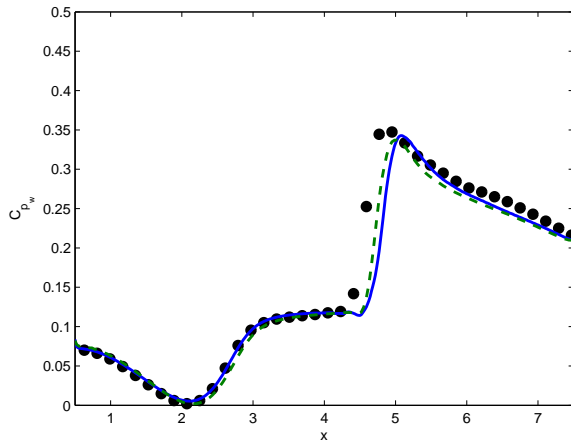


Figure 4. Coefficient of pressure at the wall for CTR simulations. DNS (circles), LES with dynamic Smagorinsky model (line), and UDNS (dashed line).

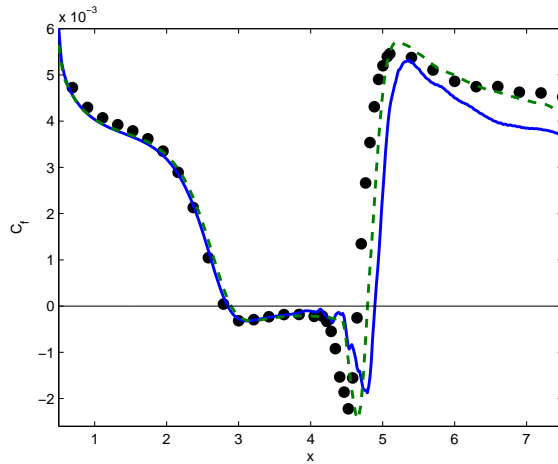


Figure 5. Wall coefficient of friction for CTR simulations. DNS (circles), LES with dynamic Smagorinsky model (line), and UDNS (dashed line).

region. The suction side (a line below the zero line) shows similar deficiencies as the pressure plot, i.e., the main features of the secondary separation around mid-cord are not well resolved. However, the overall length of the bubble is adequately predicted even though the bubble appears to be shifted slightly downstream.

The same geometry as for INCA has been used in simulations performed with the commercial code STAR-CCM+, except for the sharp trailing edge which could not be retained. To have a grid similar to the grid used in INCA a tetrahedral grid for the outer flow is used with a boundary fitted grid around the airfoil. Three simulations have been performed. An under-resolved DNS (without an LES model) and two simulations with *explicit* LES models available in the code: WALE and the Dynamic Smagorinsky model (only results for the latter model are shown as no significant differences between both models were observed). A quantitative comparison for the pressure coefficient is shown in Fig. 6. All cases behave similarly, doing a good job on both pressure and suction side and they are able to capture the secondary peak at mid-cord on the suction side. A good quantitative performance of the sim-

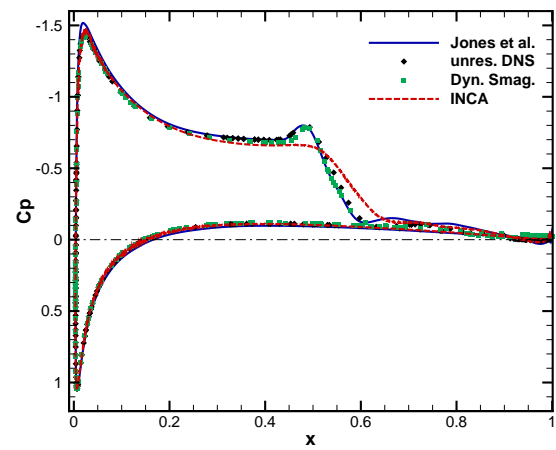


Figure 6. 2-D pressure coefficient at the wall for NACA-0012 airfoil simulations. DNS Jones *et al.* (2008) (solid blu line), STAR-CCM+ UDNS (black diamonds), STAR-CCM+ Dynamic Smagorinsky (green squares), and INCA (dashed red line).

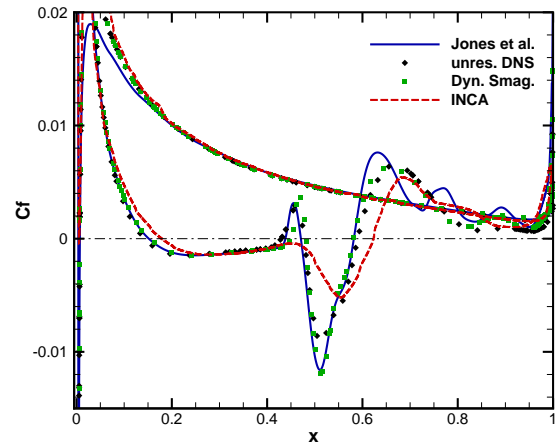


Figure 7. 2-D Wall coefficient of friction for NACA-0012 airfoil simulations. DNS Jones *et al.* (2008) (solid blue line), STAR-CCM+ UDNS (black diamonds), STAR-CCM+ Dynamic Smagorinsky (green squares), and INCA (dashed red line).

ulations is further confirmed by the skin friction coefficient results shown in Fig. 7. For the pressure side the differences are negligible across the length of the airfoil. For the suction side all relevant features observed in DNS are captured, including the magnitude of the secondary separation peak at mid-cord. Interestingly, even under-resolved DNS, does a very good job overall, slightly underestimating the negative peak and slightly overestimating the reattachment point.

DISCUSSION AND CONCLUSIONS

The good quantitative agreement between the no-model, highly under-resolved DNS and benchmark DNS results for the flat plate case suggests that the code used may belong to a category of implicit LES (ILES) where the numerical dissipation plays the role of sub-grid scale (SGS) models. As is evident in the results presented in Figs. 4 and 5, the addition of a SGS model, even when coupled with

August 28 - 30, 2013 Poitiers, France

higher resolution, visibly worsens agreement with the DNS benchmark compared to the no-model case. Such behavior is expected for codes that already provide enough dissipation through their numerics so that additional explicit SGS dissipation is not required. This claim has been substantiated by an analysis presented by Cadieux *et al.* (2013) where numerical dissipation effects were quantified using techniques developed by Domaradzki *et al.* (2003); Domaradzki & Radhakrishnan (2005); Bogey & Bailly (2006); Diamessis *et al.* (2008). Similarly, it is interesting to note the good performance of the commercial code STAR-CCM+ for the under-resolved DNS case. This also suggests that the numerical dissipation in the commercial code is substantial and may be comparable to the SGS dissipation provided by the explicit SGS models.

The capability to predict accurately and at low computational cost the average skin friction, pressure coefficient, and the location of separation and reattachment is of particular interest to airfoil and blade designers. In this work such capability has been demonstrated for simulations of laminar separation bubble flows at moderate Reynolds numbers using several different codes and a resolution on the order of 1% of their fully-resolved 3-D DNS counterparts. It appears that the observed good agreement with highly resolved DNS is at least partially attributable to the presence of the numerical dissipation in typical engineering codes used for simulating such flows.

REFERENCES

- Alam, M. & Sandham, N.D. 2000 Direct numerical simulation of 'short' laminar separation bubbles with turbulent reattachment. *J. Fluid Mech.* **410**, 1–28.
- Almutairi, J. H., Jones, L. E. & Sandham, N. D. 2010 Intermittent bursting of a laminar separation bubble on an airfoil. *AIAA J.* **48** (2), 414–426.
- Bogey, C. & Bailly, C. 2006 Large eddy simulations of transitional round jets: Influence of the Reynolds number on flow development and energy dissipation. *Phys. Fluids* **18** (6), 065101.
- Cadieux, F., Domaradzki, J. A., Sayadi, T. & Bose, T. 2013 DNS and LES of laminar separation bubbles at moderate Reynolds numbers. *ASME J. Fluids Eng.* **in press**.
- CD-adapco 2013 STAR-CCM+ manual. Version 8.02.
- Diamessis, P.J., Lin, Y.C. & Domaradzki, J. A. 2008 Effective numerical viscosity in spectral multidomain penalty method-based simulations of localized turbulence. *J. Comput. Phys.* **227**, 8145–8164.
- Domaradzki, J. A. & Radhakrishnan, S. 2005 Effective eddy viscosities in implicit modeling of decaying high Reynolds number turbulence with and without rotation. *Fluid Dyn. Res.* **36**, 385–406.
- Domaradzki, J. A., Xiao, Z. & Smolarkiewicz, P. K. 2003 Effective eddy viscosities in implicit large eddy simulations of turbulent flows. *Phys. Fluids* **15** (12), 3890–3893.
- Eisenbach, S. & Friedrich, R. 2008 Large-eddy simulation of flow separation on an airfoil at a high angle of attack and $Re = 10^5$ using Cartesian grids. *Theor. Comp. Fluid Dyn.* **22**, 213–225, 10.1007/s00162-007-0072-z.
- Germano, M., Piomelli, U., Moin, P. & Cabot, W. H. 1991 A dynamic subgrid-scale eddy viscosity model. *Phys. Fluids A* **3**, 1760–1765.
- Grilli, M., Hickel, S., Hu, X.Y. & Adams, N.A. 2009 Conservative immersed boundary method for compressible flows. Academy Colloquium on Immersed boundary methods: current status and future research directions, Amsterdam, The Netherlands.
- Hain, R., Kähler, C. J. & Radespiel, R. 2009 Dynamics of laminar separation bubbles at low-Reynolds-number aerofoils. *J. Fluid Mech.* **630**, 129–153.
- Hickel, S., Adams, N.A. & Domaradzki, J.A. 2006 An adaptive local deconvolution method for implicit LES. *J. Comp. Phys.* **213**, 413–436.
- Hickel, S. & Larsson, J. 2008 An adaptive local deconvolution model for compressible turbulence. In *Proceedings of the Summer Program*, p. 85.
- Hu, H., Yang, Z. & Igarashi, H. 2007 Aerodynamic hysteresis of a low-Reynolds-number airfoil. *J. Aircraft* **44** (6), 2083–2085.
- Jones, L.E., Sandberg, R.D. & Sandham, N.D. 2010 Stability and receptivity characteristics of a laminar separation bubble on an aerofoil. *J. Fluid Mech.* **648**, 257–296.
- Jones, L. E., Sandberg, R. D. & Sandham, N. D. 2008 Direct numerical simulations of forced and unforced separation bubbles on an airfoil at incidence. *J. Fluid Mech.* **602**, 175–207.
- Lele, S. K. 1992 Compact finite difference schemes with spectral like resolution. *J. Comput. Phys.* **103**, 16–42.
- Lilly, D.K. 1992 A proposed modification of the Germano subgrid-scale closure method. *Phys. Fluids A* **4**, 633–635.
- Lin, J. C. M. & L.Pauley, L. 1996 Low-Reynolds-number separation on an airfoil. *AIAA J.* **34** (8), 1570–1577.
- Lodato, G., Domingo, P. & Vervisch, L. 2008 Three-dimensional boundary conditions for direct and large-eddy simulation of compressible viscous flows. *J. Comp. Phys.* **227** (10), 5105–5143.
- Mani, Ali 2012 Analysis and optimization of numerical sponge layers as a nonreflective boundary treatment. *J. Comput. Phys.* **231** (2), 704 – 716.
- Marxen, O., Lang, M. & Wagner, S. 2003 A combined experimental/numerical study of unsteady phenomena in a laminar separation bubble. *Flow, Turbul. Combust.* **71**, 133–146.
- Marxen, O. & Rist, U. 2010 Mean flow deformation in a laminar separation bubble: separation and stability characteristics. *J. Fluid Mech.* **660**, 37–54.
- Meyer, M., Devesa, A., Hickel, S., Hu, X.Y. & Adams, N.A. 2010 A conservative immersed interface method for Large-Eddy Simulation of incompressible flows. *J. Comp. Phys.* **229** (18), 6300–6317.
- Nagarajan, S. 2004 Leading edge effects in bypass transition. PhD thesis, Stanford University.
- Nagarajan, S., Lele, S. K. & Ferziger, J. H. 2007 Leading-edge effects in bypass transition. *J. Fluid Mech.* **572**, 471–504.
- Nicoud, F. & Ducros, F. 1999 Subgrid-scale stress modelling based on the square of the velocity gradient. *Flow Turbul. Combust.* **62** (3), 183–200.
- Poinsot, T. J. & Lele, S.K. 1992 Boundary conditions for direct simulations of compressible viscous flows. *J. Comp. Phys.* **101** (1), 104–129.
- Spalart, P.R. & Strelets, M.K. 2000 Mechanisms of transition and heat transfer in a separation bubble. *J. Fluid Mech.* **403**, 329–349.
- Spedding, G.R. & McArthur, J. 2010 Span efficiencies of wings at low Reynolds numbers. *J. Aircraft* **47** (1), 120–128.
- Wilson, P.G. & Pauley, L.L. 1998 Two- and three-



August 28 - 30, 2013 Poitiers, France

dimensional large-eddy simulations of a transitional separation bubble. *Phys. Fluids* **10**, 2932–2940.
Yang, Z. & Voke, P.R. 2001 Large-eddy simulation of

boundary-layer separation and transition at a change of surface curvature. *J. Fluid Mech.* **439**, 305–333.